REPORT DOCUMENTATION PAGE

Form Approved
OMB No. 0704-0188

1. REPORT DATE *(DD-MM-YYYY)*	2. REPORT TYPE	3. DATES COVERED *(From - To)*
11 February 2003	Technical Paper	

4. TITLE AND SUBTITLE

On the Existence of FN_5, a Theoretical and Experimental Study

5a. CONTRACT NUMBER

5b. GRANT NUMBER

5c. PROGRAM ELEMENT NUMBER

6. AUTHOR(S)

[1]Heather M. Netzloff, Mark S. Gordon

[2]Karl Christe, William W. Wilson, Ashwani Vij, Vandana Vij, Jerry A. Boatz

5d. PROJECT NUMBER
DARP

5e. TASK NUMBER
A205

5f. WORK UNIT NUMBER

7. PERFORMING ORGANIZATION NAME(S) AND ADDRESS(ES)

[1]Department of Chemistry
Iowa State University
Ames, IA 50011

[2]Air Force Research Laboratory
ERC
10 E. Saturn Blvd.
Edwards AFB, CA 93524-7680

8. PERFORMING ORGANIZATION REPORT NUMBER

AFRL-PR-ED-TP-2003-035

9. SPONSORING / MONITORING AGENCY NAME(S) AND ADDRESS(ES)

Air Force Research Laboratory (AFMC)
AFRL/PRS
5 Pollux Drive
Edwards AFB CA 93524-7048

10. SPONSOR/MONITOR'S ACRONYM(S)

11. SPONSOR/MONITOR'S NUMBER(S)
AFRL-PR-ED-TP-2003-035

12. DISTRIBUTION / AVAILABILITY STATEMENT

Approved for public release; distribution unlimited.

13. SUPPLEMENTARY NOTES

14. ABSTRACT

15. SUBJECT TERMS

16. SECURITY CLASSIFICATION OF:			17. LIMITATION OF ABSTRACT	18. NUMBER OF PAGES	19a. NAME OF RESPONSIBLE PERSON
					Sheila Benner
a. REPORT	b. ABSTRACT	c. THIS PAGE	A		19b. TELEPHONE NUMBER *(include area code)*
Unclassified	Unclassified	Unclassified			(661) 275-5693

FILE

MEMORANDUM FOR PRS (In-House Publication)

FROM: PROI (STINFO) 11 Feb 2003

SUBJECT: Authorization for Release of Technical Information, Control Number: **AFRL-PR-ED-TP-2003-035** Heather M. Netzloff and Mark S. Gordon (Iowa St. Univ.); Karl Christe; William W. Wilson; Ashwani Vij; Vandana Vij; Jerry A. Boatz (AFRL/PRSP), "On the Existence of FN_5, a Theoretical and Experimental Study"

Dr. Corley 55881

Dr. Christe 55194

Journal of Chemical Physics **(Statement A)**

On the Existence of FN_5, a Theoretical and Experimental Study

Heather M. Netzloff and Mark S. Gordon*

Department of Chemistry Iowa State University, Ames, IA 50011

Karl Christe,* William W. Wilson, Ashwani Vij, Vandana Vij, and Jerry A. Boatz

Air Force Research Laboratory, Edwards AFB, CA 93524, and Loker Research Institute, University of Southern California, Los Angeles, CA 90089

Abstract

The possible existence of FN_5 was studied by *ab initio* electronic structure theory. Calculations were carried out at the MP2/6-31+G(d) and CCSD(T)/aug-cc-pVDZ levels of theory for the $N_5^+AsF_6^-$ ion pair and its decomposition to FN_5 and AsF_5. Six different vibrationally stable isomers of FN_5 were identified. Intrinsic reaction coordinate (IRC) and dynamic reaction path (DRP) calculations were used to study the isomerization of FN_5 and its decomposition to FN_3 and N_2. A Rice-Ramsperger-Kassel-Marcus (RRKM) analysis was performed, indicating upper limits to the lifetimes of the FN_5 isomers in the nanosecond range. These theoretical predictions were confirmed by an experimental study of the thermolyses of N_5AsF_6 and $[N_5]_2SnF_6$ and the displacement of FN_5 from N_5SbF_6 with CsF, using FT-IR spectroscopy. In accord with the theoretical predictions, the primary reaction product FN_5 could not be observed, but its decomposition products FN_3, F_2N_2, and NF_3 were identified.

Introduction

Polynitrogen compounds are of great interest as high energy density materials (HEDM).[1-5] Although theoretical studies have predicted numerous kinetically stable polynitrogen compounds,[4] almost all attempts to synthesize them have failed due to their very high endothermicities, low energy barriers towards decomposition, and a lack of suitable synthetic methods. The high energy content of polynitrogen compounds arises from an unusual property of nitrogen that sets it apart from most other chemical elements. Its single and double bond energies

are considerably less than one-third and two-thirds, respectively, of its triple bond energy. Therefore, the decomposition of polynitrogen species to N_2 is accompanied by a large release of energy.[1]

Recently, the N_5^+ cation has been synthesized and characterized.[1,2] It represents only the second known homonuclear polynitrogen species after N_3^-,[6] that is stable and can be prepared on a macroscopic scale. Its bent structure of C_{2v} symmetry (Figure 1) was established by a crystal structure determination of $N_5^+Sb_2F_{11}^-$ and vibrational and NMR spectroscopy, and is in accord with *ab initio* and density functional theory (DFT) calculations.[1,2,7] The bent structure avoids the unfavorable neighboring positive charges that would result from a linear structure.[1]

Most salts consisting of an X^+ cation and a complex fluoro anion, MF_6^-, are prepared by the transfer of an F^- anion from the parent FX molecule to the strong Lewis acid MF_5 (eq. 1).

$$FX + MF_5 \Leftrightarrow X^+MF_6^- \qquad (1)$$

Usually this reaction is reversible and the FX molecule can be regenerated by either thermolysis of $X^+MF_6^-$ or a displacement reaction between $X^+MF_6^-$ and a stronger Lewis base, such as CsF (eq. 2).

$$X^+MF_6^- + CsF \Rightarrow FX + CsMF_6 \qquad (2)$$

Only a few $X^+MF_6^-$ salts are known for which FX cannot be generated in this manner. Typical examples are the NF_4^+,[8] ClF_6^+,[9] and BrF_6^+[10] salts where the corresponding FX parent compounds cannot exist because the maximum coordination number of the central atom would be exceeded.[11] The reverse case, where an amphoteric FX molecule exists but the corresponding X^+ cation does not, is also known but rare. A typical example is FN_3 that does not form a stable N_3^+ salt with strong Lewis acids.[12]

The availability of several marginally stable N_5^+ salts, such as $N_5^+AsF_6^-$,[1] $N_5^+SbF_6^-$,[2] and $[N_5]^+_2[SnF_6]^{2-}$ [13] that can be readily subjected to thermolysis or displacement reactions, offered an ideal opportunity to probe the possible existence of the unknown FN_5 molecule. While carrying out the theoretical study, we have also investigated the potential energy surfaces of the $N_5^+AsF_6^-$ ion pair and its FN_5 decomposition product in order to better understand the likely structure and stability of this new polynitrogen species.

Experimental Section

Caution! Reactions of N_5^+ salts can be violent and can result in explosions,[1,2] particularly when highly shock sensitive FN_3[12,14] is formed as a decomposition product. Therefore, these materials should be handled only on a small scale with appropriate safety precautions (face shield, leather gloves, and protective clothing).

Materials and Apparatus. All reactions were carried out in a demountable Teflon-PFA condensing side arm of a 5 cm path length, Teflon-FEP infrared cell equipped with AgCl windows. Nonvolatile solids were loaded in the dry nitrogen atmosphere of a glove box into the side arm of the IR cell. The cell was then evacuated and placed into the FT-IR spectrometer. The decomposition or displacement reactions were initiated by gentle warming, and the volatile decomposition products were continuously monitored by infrared spectroscopy using a Mattson Galaxy FT-IR spectrometer. Volatile materials were handled on a stainless steel/Teflon-FEP vacuum line.[15]

The $N_5^+AsF_6^-$,[1] $N_5^+SbF_6^-$,[2] and $[N_5]^+_2[SnF_6]^{2-}$[13] starting materials were prepared by literature methods. The CsF (KBI) was fused in a platinum crucible, transferred while hot into the dry box, and finely powdered.

Computational Methods

Initial optimizations of all structures were performed using second order perturbation theory (MP2)[16] and the 6-31+G(d) basis set.[17] Hessians (energy second derivatives) were calculated for the final equilibrium structures to determine if they are minima (positive definite hessian) or transition states (one negative eigenvalue). At the final MP2/6-31+G(d) geometries, improved relative energies were obtained using singles and doubles coupled cluster theory with triples included perturbatively (CCSD(T))[18] and the aug-cc-pVDZ basis set.[19] The MP2 calculations were performed using the electronic structure code GAMESS,[20] while the CCSD(T) calculations were carried out using ACES II.[21]

Intrinsic reaction coordinate (IRC) pathways[22] were employed in the study of the FN_5 species in order to connect isomer minima, transition states, and decomposition products. The IRC method is the minimum energy path (MEP) in mass weighted Cartesian coordinates. IRC calculations were performed with GAMESS using the second-order method developed by

Gonzalez and Schlegel[23] with a step size of 0.1 (amu)$^{1/2}$-bohr.

A simple Rice-Ramsperger-Kassel-Marcus (RRKM) analysis was performed on the isomers included in the potential energy surfaces obtained with the IRC calculations. The RRKM theory of reaction dynamics can be used to give an upper limit to the lifetime of the minima.[24] It assumes a microcanonical equilibrium and a locally separable reaction coordinate. The microscopic rate constant is proportional to the sum of states of the ith reaction channel (W_N^i (E – E_0^i)) divided by the reaction density of states (ρ_N):

$$k \propto W_N^i (E - E_0^i) / \rho_N (E) \qquad (3)$$

$$k = \frac{\prod_{i=1}^{3N-6} \nu_i}{\prod_{i=1}^{3N-7} \nu_i^{TS}} \left(\frac{E - E_0^{barrier}}{E} \right)^{3N-7} \qquad (4)$$

where k = rate constant

ν_i = ith frequency of the minima

ν_i^{TS} = ith frequency of the transition state

E = applied energy

$E_0^{barrier}$ = barrier energy

Note that the lifetime $\tau = 1 / k$.

Finally, in order to further study the decomposition and stability of several FN_5 isomers, the dynamic reaction path (DRP) method was used to add photons (kinetic energy (KE)) to one or more FN_5 vibrational normal modes.[25] The DRP method, a classical trajectory approach, is based on a quantum chemical potential energy surface (PES) that need not be known ahead of time. Unlike the IRC, energy is strictly conserved along the dynamic reaction path. Thus, larger step sizes can be used. In this way a classical trajectory is developed "on-the-fly" without prior knowledge of the PES. GAMESS can use normal modes as the initial dynamic reaction coordinates. An initial KE and velocity direction is supplied to one or more modes (in units of quanta).[26] The strategy is to provide energy to those modes that appear to lead to desired reaction

products. Because there is often significant mode-mode mixing, the applied energy is usually in excess of the reaction/decomposition barrier. This is a direct dynamics method in that the *ab initio* (in the present case, MP2) gradients/forces are calculated at each step and are then used to solve Newton's equations of motion and propagate the system. Step sizes ranged from 0.1 to 0.2 fs, depending on how well energy conservation criteria were satisfied.

Results and Discussion

The $N_5^+AsF_6^-$ Ion Pair. The starting points for the calculations were the AsF_6^- and N_5^+ ions separated by a distance of ~10.0 Å, in C_1 symmetry, followed by a complete geometry optimization. The resulting ion pair is shown in Figure 2a. At the MP2/6-31+G(d) level of theory, the ion pair is 98.8 kcal/mol lower in energy than the separated ions (Table 1).

MP2 Mulliken charges on the N_5^+ and AsF_6^- units within the ion pair show that the charge separation is $\pm$0.825; thus, there is relatively little charge transfer between the ions. In comparison with the separated ions (Figures 2b and 3b), the N_5^+ unit in the ion pair has a less negative charge on the central N by approximately 0.3, while the terminal N atoms are about 0.2 less positive than in the isolated N_5^+ ion. In the case of AsF_6^- in the ion pair, all As-F bonds except for the bond opposite to the N_5^+ unit have been elongated by about 0.085 Å (Table 2). This effect can be explained by the partial removal of an electron from bonding orbitals. It is interesting to note that the bond distances in N_5^+ do not exhibit a similar effect and are essentially unchanged.

In isolated N_5^+, the central N has a large negative charge (Figure 3b). This charge is reduced by a factor of two in the ion pair. All other N atoms are positive, with the terminal N atoms being most positive. This type of charge distribution can be rationalized by the valence bond structures[1,2,27] given in Figure 1. It must be kept in mind, however, that the magnitude of the charges varies strongly with the calculation method, although their signs and relative order remain the same. Thus, at the NBO (B3LYP/aug-cc-pVDZ) level of theory, the charges on N1, N2, and N3 are significantly smaller and amount to 0.33, 0.22, and –0.11, respectively.[28]

As can be seen from Figure 2a, the closest N-F distances in the ion pair are N2-F8 = 2.26 Å and N4-F8 = 2.34 Å. They are much longer than a typical N-F bond (~1.3 Å)[29], but significantly

shorter than the sum of their Van der Waals radii (3.0 Å)[30] and the shortest N···F contacts observed in the crystal structure of $N_5^+Sb_2F_{11}^-$ (2.72 and 2.78 Å).[2]

Since there is still a large charge separation between the components of the ion pair, it is of interest to consider how much energy would be required to transfer F^- from AsF_6^- to N_5^+ to make gaseous AsF_5 and FN_5. At the MP2/6-31+G(d) level of theory, the ion pair is 46.5 kcal/mol lower in energy than the separated AsF_5 and *bifurcated(bif)*-FN_5 molecules, indicating that it takes at least this much energy to transfer F^- from AsF_6^- to N_5^+ to make *bif*-FN_5 and AsF_5 (Figure 4). Thus, the ion pair is reasonably stable to dissociation to gaseous AsF_5 and *bif*-FN_5. Because an ion pair is only a poor approximation to a crystalline solid, the 25.5 kcal/mol difference between the lattice energy of $N_5^+AsF_6^-$ (124 ± 4 kcal/mol)[31] and the ion pair energy (98.8 kcal/mol) must be added to the above minimum decomposition energy barrier of 46.5 kcal/mol when considering the thermal stability of solid N_5AsF_6. The resulting minimum decomposition energy barrier of 72.0 kcal/mol for crystalline N_5AsF_6 is in accord with the experimental observation that this salt is marginally stable at room temperature.[1] The experimentally observed irreversible decomposition of N_5AsF_6 at higher temperatures[1] is due to the subsequent rapid, highly exothermic, and irreversible decompositions of FN_5 and FN_3 (see below).

In addition to the $[AsF_6]^-[N_5]^+$ structure discussed above, a geometry search revealed a second, lower energy isomer. This C_{2v} structure is obtained from the structure show in Figure 2a by rotating the $[AsF_6]^-$ anion so that the As_6, F_7, and F_8 atoms are coplanar with $[N_5]^+$. The C_2 rotation axis then passes through atoms N_3 and As_6. The second symmetry plane contains N_3, As_6, and F_9-F_{12} with F_9 and F_{11} pointing towards the $[N_5]^+$ cation and F_{10} and F_{12} pointed away from it. Some of the distinguishing features of this C_{2v} geometry are the As-F distances (As-$F_{7,8}$ = 1.75 Å; As-$F_{9,11}$ = 1.81 Å; As-$F_{10,12}$ = 1.72 Å); the N_1-F_8 (N_5-F_7) distance is 2.80 Å. The F_9-N_2, F_9-N_4, F_{11}-N_2, and F_{11}-N_4 distances are each 2.47 Å. The geometry of the $[N_5]^+$ cation is virtually identical to that in Figure 2a. This second bifurcated isomer is ~10 kcal/mol lower in energy than the structure shown in Figure 2a, most likely because of the electrostatic interactions between four F atoms with N. However, the higher energy structure is more likely to yield the neutral species $AsF_5 + FN_5$. In either case, the ion complex is clearly much lower in energy than the separated neutrals.

FN_5 Isomers. Because the F^- ion can attach itself in different ways to the three different nitrogen atoms of N_5^+, it is necessary to explore the different possible isomers of FN_5 and their relative energies and stabilities. An exhaustive study was performed and six stable isomers were found. Their relevant energies and geometries are listed in Tables 3 and 4, respectively. Optimized structures were obtained for each isomer and hessians confirmed that these structures are minima on the potential energy surface. The relevant geometrical features are summarized in Figure 5 and Table 4. The N-F and N-N bond lengths are similar for all isomers except for the bifurcated isomer (1) and the cyclic structure (6). All isomers are planar molecules. Both MP2 and CCSD(T) calculations predict the *cis-* and *cyclic*-isomers to be among the lowest energy species. Indeed, except for the bifurcated isomer, the two levels of theory predict similar relative energies (Table 3). Note that the MP2 results are not very basis set dependent. The *cis-*, *trans-*, *wag-*, and *harp-* isomers are all within a few kcal/mol of each other and can be easily interconverted by simple rotations around the N3-N4 and N4-N5 bonds. The more accurate and reliable CCSD(T) method places the bifurcated isomer 3-11 kcal/mol above the other isomers. Since the two N-F distances in this "bifurcated" isomer differ by 0.342 Å, this isomer might reasonably be described as an N_β-bonded isomer with a weak secondary interaction to the other N_β atom, while the other four non-cyclic isomers are all N_α-bonded. The formation of the cyclic isomer (6) is less likely to form in the experiments because it would probably involve a fluoride attacking N_5^+ from the backside at its central N_γ atom. Such an approach is not likely since both reacting atoms apparently carry partial negative charges that should repel each other.

Because N_2 is so stable, the dissociation of FN_5 to FN_3 and N_2 is 45.5 kcal/mol exothermic at the CCSD(T) level of theory (Table 3) and is irreversible. Therefore, it is important to explore the possible decomposition pathways for the preferred FN_5 isomers and to determine their energy barriers towards decomposition.

In order to explore both the isomerization and decomposition pathways, IRC studies were performed at the MP2 level of theory to connect minima with the corresponding transition states (TS). Transition states are illustrated in Figure 6, and FN_3 is depicted in Figure 7; detailed geometries are given in Table 5. The first IRC was started from the "bifurcated" isomer, which most closely resembles the original ion pair. Structurally, the isomer that most naturally connects with the *bifurcated*-isomer is the *harp*-isomer, since this simply requires F to move to a neighboring nitrogen atom of the N_5 moiety via TS14. Starting from *harp*, two PESs have been

identified (Figure 8) that the *harp*-isomer can take to reach decomposition products: a "direct" decomposition route (through TS4p) or an isomerization via the *cis*-isomer (through TS42). The *cis*-isomer decomposes directly to FN_3 +N_2 (through TS2p). As shown in Figure 8 and Table 6, the bottleneck for both reaction paths is the initial barrier towards isomerization from *bifurcated* to *harp* (through TS 14), predicted to be 8.9 kcal/mol. The subsequent activation energies are much smaller, so once the *harp*-isomer is reached, the decomposition to FN_3 +N_2 should proceed even more easily.

The two PESs are qualitatively similar at the MP2/6-31+G(d) and CCSD(T)/aug-cc-pVDZ levels of theory. The MP2 activation energies are larger than those from CCSD(T), and all transition states and minima, excluding the initial bifurcated species, are higher in energy than the reference *cis*-isomer. CCSD(T) predicts that all minima and TSs are higher in energy than the reference *cis*-isomer (Table 3).

The results of a *qualitative* RRKM analysis (using the vibrational frequencies in Table 7) for the two isomerization reactions and two decomposition reactions are shown in Tables 8 and 9. Several values were chosen for E, the applied energy, in equation (4) for each minimum. Since the CCSD(T) and MP2 activation energies are different (Table 6), a given value of E corresponds to different excess energies above the barrier. So, in Tables 8 and 9, a given amount of energy above a barrier corresponds to different values of E. Since the CCSD(T) energies were obtained as single energy calculations at the MP2 geometries, the frequencies used in both sets of RRKM calculations are those obtained from MP2. Thus, the CCSD(T) results are only qualitative, but these frequencies are not expected to be very different. Since the CCSD(T) barriers are much lower in energy than those based on MP2, the corresponding lifetimes will be smaller. Of course, the shorter the predicted lifetime, the more likely it is that the isomerization or dissociation will occur. At the CCSD(T) level of theory, the predicted lifetimes for the two isomerization reactions, *bifurcated* (1)→ *harp* (4) and *harp* (4)→ *cis* (2), are on the order of a few nanoseconds even in the case where an energy that is only 5 kcal/mol above the barrier is added. When this excess energy rises to 40 kcal/mol, these lifetimes decrease to 1-2 picoseconds. The lifetimes for the decomposition reactions, from *harp* and *cis* to FN_3 and N_2, are even shorter.

DRP Calculations. In order to further study the decomposition and stability of the *harp*- and *cis*-FN_5 isomers, the dynamic reaction path (DRP) method[25,26] was used to provide kinetic energy to one or more vibrational normal modes.

For the *cis*-isomer, mode 10 (Figure 9a) is a good candidate for breaking the N3-N4 bond since ν_{10} is the symmetric N3-N4-N5 stretching mode. At the MP2/6-31+G(d) level, the barrier for the decomposition, *cis*-$FN_5 \rightarrow FN_3 + N_2$, is approximately 22 kcal/mol. With the addition of approximately 35 kcal/mol to this mode, the N3-N4 bond undergoes only oscillations, and at least 51 kcal/mol of KE must be applied to this mode in order to break the N3-N4 bond (the bond breaks after 5.6 fs into such a trajectory run). Figures 10 and 11 show various structures along the trajectories with the addition of 35 and 51 kcal/mol of KE, respectively. Further illustration of this phenomenon is shown in Figure 12 where the coordinate changes in terms of the normal modes of the equilibrium structure for both E = 35 and E = 51 kcal/mol are plotted. With the addition of 35 kcal/mol, the KE is quickly redistributed to other modes. This dissipates the applied energy, so bond oscillations due to the activation of other modes result. For E = 51 kcal/mol, the energy remains localized in mode 10; the modes become well separated and do not undergo wild oscillations. There is enough energy available to "push" the N_2 fragment away so it is not recaptured during oscillations

As noted earlier, the *harp*-isomer can decompose in a direct or stepwise manner. The MP2/6-31+G(d) barrier to direct decomposition is 7.5 kcal/mol, while the barrier for the isomerization, *harp*→*cis*, is 5.4 kcal/mol. In the analysis of this structure, ν_{12} (Figure 9b) appears to be a good candidate for N3-N4 bond breaking since ν_{12} is the N4-N5 stretching mode. After the addition of 44 kcal/mol, the N3-N4 bond breaks, but it then reforms and oscillates. As in the case for the *cis*-isomer, this can be seen in the graphs of normal mode coordinate change versus time. Figure 13 shows that the energy applied to ν_{12} dissipates to other modes even more rapidly than in the case of the *cis*-isomer.

The MP2 and CCSD(T) RRKM analyses for the addition of energy, corresponding to this DRP for both the *cis*- and *harp*-isomers, are given in Table 9. The examples discussed above are in boldface in Table 9. Consider the decomposition of the *cis*-isomer, using ν_{10}. At least seven (four) vibrational quanta are required to surmount the barrier in this mode for MP2 (CCSD(T)), corresponding to lifetimes of 0.2 and 855 milliseconds, respectively. For an E value of 35 kcal/mol, corresponding to 10 vibrational quanta, the lifetimes are 216 and 0.9 ps, respectively.

The trajectory with E = 35 kcal/mol was only run for ~ 0.15 ps, and only bond oscillations were observed. For E = 52 kcal/mol (15 quanta), the predicted lifetimes 116 fs and 1.7 ps for CCSD(T) and MP2, respectively. The E = 52 kcal/mol trajectory shows complete bond dissociation after ~ 6 fs (0.006 ps). For the *harp*-isomer, the addition of E = 44 kcal/mol to mode 12 (7 quanta) shows no dissociation after ~ 600 fs (0.6 ps). Upper limit lifetimes for this isomer, depending on whether one is considering the isomerization or decomposition channel, are ~ 3 ps and 0.3 ps, respectively, at the MP2 level and 1.9 ps and 50.4 fs, respectively, at the CCSD(T) level. It is important to reiterate here the following point: the reason that the amount of energy required to cause dissociation in the DRP trajectories exceeds the calculated barrier heights is that the energy provided to a specific vibrational mode does not localize in the bond that breaks in the reaction.

Experimental Results. The vacuum thermolyses of $N_5^+AsF_6^-$ (eq. 5) and $[N_5]^+_2[SnF_6]^{2-}$ (eq. 6), and the displacement reaction between CsF and $N_5^+SbF_6^-$ (eq. 7) were studied experimentally by fast, *in situ* FT-IR spectroscopy of the gaseous reaction products.

$$N_5^+AsF_6^- \rightarrow [FN_5] + AsF_5 \quad (5)$$

$$(N_5)^+_2SnF_6^{2-} \rightarrow [FN_5] + N_5^+SnF_5^- \quad (6)$$

$$N_5^+SbF_6^- + CsF \rightarrow [FN_5] + CsSbF_6 \quad (7)$$

In excellent agreement with the above theoretical lifetime predictions for FN_5, this molecule could not be observed directly; however its expected decomposition products (eq. 8-11) were observed.

$$[FN_5] \rightarrow FN_3 + N_2 \quad (8)$$

$$FN_3 \rightarrow [FN] + N_2 \quad (9)$$

$$2\,[FN] \rightarrow F_2N_2 \quad (10)$$

$$3\,F_2N_2 \rightarrow 2\,NF_3 + 2\,N_2 \quad (11)$$

Because reactions 8-11 are all strongly exothermic, the thermodynamically most stable products, NF_3 and N_2,[32] were obtained as the major final products. However, the formation of smaller amounts of FN_3 and F_2N_2 was also observed, thus confirming the above sequence of reactions.

Conclusions

In contrast to FN_3 that can be isolated at room temperature but does not form stable N_3^+ salts with strong Lewis acids,[12] N_5^+ salts are stable but their FN_5 parent molecule has very limited kinetic stability. Because of the general difficulty of correctly modeling infinite crystal lattices,[33] the ion pair $N_5^+AsF_6^-$ and its dissociation products were studied. It is shown that at the MP2/6-31+G(d) level the ion pair and crystalline $N_5^+AsF_6^-$ are more stable than the free FN_5 and AsF_5 molecules by 46.5 and 72.0 kcal/mol, respectively. These values represent minimum dissociation energy barriers; the latter value is in accord with the observed marginal stability of crystalline $N_5^+AsF_6^-$ at room temperature. The FN_5 molecule can exist as at least six different, vibrationally stable isomers (one cyclic, one bifurcated, and four chain-like structures) that differ in energy by only 6.4, 9.0, and 11.2 kcal/mol at the MP2/6-31+G(d), MP2/aug-cc-pVDZ, and CCSD(T)/aug-cc-pVDZ levels, respectively. Decomposition studies of FN_5 reveal two distinct pathways to $FN_3 + N_2$. The energy change from the initial bifurcated FN_5 isomer to $FN_3 + N_2$ is predicted to be 56.0 kcal/mol at the CCSD(T) level of theory.

IRC, DRP, and RRKM calculations suggest that the energy barriers for these decomposition pathways are very low resulting in predicted life times for FN_5 at room temperature on the order of nanoseconds. These predictions of an extremely short lived FN_5 are confirmed by our experimental FT-IR studies on the thermolyses of $N_5^+AsF_6^-$ and $[N_5]^+_2[SnF_6]^{2-}$, and the displacement reaction between CsF and $N_5^+SbF_6^-$ which showed only the expected decomposition products FN_3, F_2N_2, and NF_3, but no evidence for the intermediate FN_5.

Acknowledgements

This work was supported by a grant (to MSG) from the Air Force Office of Scientific Research (AFOSR) and by a Grand Challenge grant of computer time from the High Performance Computing Modernization Program (to MSG and JAB) at the High Energy Maui High Performance Computation Center. The authors also thank Dr. Galina Chaban and Prof. William Hase for insightful discussions about the DRP calculations. HMN was supported by a Department of Energy Computational Science Graduate Fellowship and a Miller Fellowship from the Iowa State University Department of Chemistry. The work at the Air Force Research Laboratory was supported by the Defense Advanced Research Projects Agency (DARPA) and

AFOSR, while that at USC was supported by DARPA, AFOSR, and the National Science Foundation. The authors thank Prof. Jenkins for the lattice energy estimate for N_5AsF_6 and Drs. R. Corley, M. Berman, and D. Woodbury for their steady support. The calculations described here were performed on both local Iowa State University/DOE Ames Laboratory workstations, as well as computers at the Maui High Performance Computation Center.

References

(1) Christe, K.O.; Wilson, W.W.; Sheehy, J.A.; Boatz, J.A. *Angew. Chem. Int. Ed.* **1999**, *38*, 2004.

(2) Vij, A.; Wilson, W.W.; Vij, V.; Tham, F.S.; Sheehy, J.A.; Christe, K.O. *J. Am. Chem. Soc.* **2001**, *123*, 6308.

(3) Lauderdale, W.J.; Stanton, J.F.; Bartlett, R.J. *J.Phys. Chem.* **1992**, *96*, 1173.

(4) Glukhovtsev, M.N.; Jiao, H.; Schleyer, P.v.R. *Inorg. Chem.* **1996**, *35*, 7124.

(5) Bartlett, R. J. *Chem. Ind.-London* **2000**, *4*, 140.

(6) Curtius, T. *Ber. Dtsch. Chem. Ges.* **1890**, *23*, 3023.

(7) Pyyko, P.; Runeberg, N. *J. Mol. Struct. (Theochem.)* **1991**, *234*, 279.

(8) (a) Christe, K. O.; Guertin, J. P.; Pavlath, A. E. *Inorg. Nucl. Chem. Lett.* **1966**, *2*, 83; (b) Guertin, J. P.; Christe, K. O.; Pavlath, A. E. *Inorg. Chem.* **1966**, *5*, 1921; (c) Tolberg, W. E.; Rewick, R. T.; Stringham, R. S. *Inorg. Chem.* **1967**, *6*, 1156.

(9) (a) Christe, K. O. *Inorg. Nucl. Chem. Lett.* **1972**, *8*, 741; (b) Robero, F. Q. *Inorg. Nucl. Chem. Lett.* **1972**, *8*, 737; (c) Christe, K. O. *Inorg. Chem.* **1973**, *12*, 1580.

(10) (a) Gillespie, R. J.; Schrobilgen, G. J. *J. Chem. Soc., Chem. Commun.* **1974**, 90; (b) Gillespie, R. J.; Schrobilgen, G. J. *Inorg. Chem.* **1974**, 13, 1230; Christe, K. O. ; Wilson, R. D. *Inorg. Chem.* **1975**, *14*, 694.

(11) (a) Christe, K. O.; Wilson, W. W.; Schrobilgen, G. J.; Chiracal, R. V. *Inorg. Chem.* **1988**, *27*, 789; (b) Christe, K. O.; Wilson, W. W. *J. Am. Chem. Soc.* **1992**, *114*, 9934.

(12) Schatte, G.; Willner, H. Z. *Naturforsch.* **1991**, *46b*, 483.

(13) Wilson, W.W.; Vij, A.; Vij, V.; Christe, K.O. to be published.

(14) Gholivand, K.; Schatte, G.; Willner, H. Z. *Inorg. Chem.* **1987**, *26*, 2137.

(15) Christe, K. O.; Wilson, W. W.; Schack, C. J.; Wilson, R. D. *Inorg. Synth.* **1986**, *24*, 39.

(16) Moller, C.; Plesset, M. S. *Phys. Rev.* **1934**, *46*, 618.

(17) Hehre, W. J.;Ditchfield, R.; Pople, J. A. *J. Chem. Phys.* **1972**, *56*, 2237.

(18) Raghavachari, K.; Trucks, G. W.; Pople, J. A.; Head-Gordon, M. *Chem. Phys. Lett.* **1989**,*157*, 479.

(19) Dunning, T. H. *J. Chem. Phys.* **1989**, *90*, 1007.

(20) Schmidt, M. W.; Baldridge, K. K.; Boatz, J. A.; Elbert, S. T.; Gordon, M. S.; Jensen, J. H.; Koseki, S.; Matsunaga, N.; Nguyen, K. A.; Su, S.; Windus,

T. L. *J.Comput. Chem.* **1993**, *14*, 1347.

(21) ACES II is a program product of the Quantum Theory Project, University of Florida. Authors: Stanton, J. F.; Gauss, J.; Watts, J. D.; Nooijen, M.; Oliphant, N.; Perera, S. A.; Szalay, P. G.; Lauderdale, W. J.; Kucharski, S. A.; Gwaltney, S. R.; Beck, S.; Balková, A.; Bernholdt, D. E.; Baeck, K. K.; Rozyczko, P.; Sekino, H.; Hober, C.; Bartlett, R. J. Integral packages included are VMOL (Almlöf, J.; Taylor, P. R.); VPROPS (Taylor, P. R.) ABACUS; (Helgaker, T.; Jensen, H. J. Aa.; Jørgensen, P.; Olsen, J.; Taylor, P. R.).

(22) Garrett, B.C.; Redmon, M.; Steckler, R.; Truhlar, D.G.; Baldridge, K. K.; Bartol, D.; Schmidt, M.W.; Gordon, M.S. *J. Phys. Chem.* **1988**, *92*, 1476.

(23) Gonzales, C.; Schlegel, H. B. *J.Chem.Phys.* **1989**, *90*, 2154.

(24) (a) Robinson, P. J.; Holbrook, K. A. Unimolecular Reactions; Wiley-Interscience: New York, 1972; (b) Forst, W. Theory of Unimolecular Reactions; Academic Press: New York, 1973; (c) Schranz, H. W.; Nordholm, S.; Freasier, B. C. *Chem. Phys.* **1986**, *108*, 69.

(25) (a) Stewart, J. J. P.; Davis, L. P.; Burggraf, L. W. *J.Comput.Chem.* **1987**, *8*, 1117. (b) Maluendes, S. A.; Dupuis, M. *J. Chem. Phys.* **1990**, *93*, 5902.

(26) (a) Taketsugu, T.; Gordon, M. S. *J. Phys. Chem.* **1995**, *99*, 8462. (b) Gordon, M. S.; Chaban, G.; Taketsugu, T. *J.Phys.Chem.* **1996**, *100*, 11512.

(27) Harcourt, R. D.; Klapoetke, T. M. *Z. Naturforsch.* **2002**, *57b*, 983.

(28) Fau, S.; Bartlett, R. J. *J. Phys. Chem. A* **2001**, *105*, 4096.

(29) (a) Christe, K. O.; Lind, M. D.; Thorup, N.; Russell, D. R.; Fawcett. J. *Inorg. Chem.* **1988**, *27*, 2450; (b) Vij, A.; Zhang, X.; Christe, K. O. *Inorg. Chem.* **2001**, *40*, 416, and references cited therein.

(30) Bondi, A. *J. Phys. Chem.* **1964**, *68*, 441.

(31) Jenkins, H. D. B. private communication.

(32) Gmelin Handbook, F Suppl. Vol. 4, pg.385.

(33) Christe, K. O.; Zhang, X.; Sheehy, J. A.; Bau, R. *J. Am. Chem. Soc.* **2001**, *123*, 6338.

Table 1. Energies (hartrees), zero point energy (ZPE) corrections, and relative energies (kcal/mol) for ion pair, separated ions, and separated neutrals

Reference = ion pair

Molecule	E(MP2/6-31+G(d))	ZPE(kcal/mol)	Relative Energy[a]
$N_5^+AsF_6^-$	-3102.913474	23.3	0
N_5^+	-272.602102	12.4	--
AsF_6^-	-2830.15549	9.9	--
$N_5^+ + AsF_6^-$	-3102.757592	22.3	98.8
FN_5 (bifurcated)	-372.481754	14.0	--
AsF_5	-2730.358788	8.6	--
$FN_5 + AsF_5$	-3102.840542	22.6	46.5

*Energy in hartrees, Relative energy in kcal/mol

a. Includes ZPE correction

Table 2. Bond distances and angles for ion complex and separated ions (refer to Figures 2a and 3a).

Ion Complex

	Distances (A)		Angles (degrees)
N1-N2	1.144	N2-N3-N4	113.56
N2-N3	1.305	F10-As6-F8	86.88
N3-N4	1.312		
N4-N5	1.144		
As6-F7	1.722		
As6-F8	1.843		
As6-F9	1.843		
As6-F10	1.843		
As6-F11	1.843		
As6-F12	1.843		
N1-F8	2.720		
N2-F8	2.258		
N3-F8	2.737		
N4-F8	2.338		
N5-F8	2.879		

N_5^+

	Distances (A)		Angles (degrees)
N1-N2	1.143	N2-N3-N4	110.17
N2-N3	1.313	N1-N2-N3	167.15
N3-N4	1.313		
N4-N5	1.143		

AsF_6^-

	Distances (A)		Angles (degrees)
As-F	1.758	F-As-F	90.0

Table 3. Energies (hartrees), ZPE corrections (kcal/mol), and energies relative to the cis (2) isomer (kcal/mol) for FN_5 isomers, transition states, and decomposition products, FN_3 + N_2

Molecule	E(MP2/G)[a]	ZPE	E(CCSD(T))[b]	ΔE(MP2/G)[d]	ΔE(CCSD(T))[d]	ΔE(MP2/aug)[c,d]
bifurcated (1)	-372.48175	14.0	-372.62048	-1.1	10.5	-1.4
cis (2)	-372.47998	14.0	-372.63717	0	0	0
trans (3)	-372.47509	14.0	-372.63252	3.1	2.9	3.3
harp (4)	-372.47275	13.5	-372.62892	4.0	4.7	3.7
wag (5)	-372.47104	13.7	-372.62794	5.3	5.5	4.8
cyclic (6)	-372.48349	15.7	-372.64098	-0.5	-0.7	-4.2
TS2p[e]	-372.44101	11.3	-372.61175	21.8	13.2	21.6
TS14[e]	-372.45042	13.1	-372.6048	17.6	19.4	16.7
TS42[e]	-372.46467	13.8	-372.62343	9.4	8.4	9.2
TS4p[e]	-372.45809	11.8	-372.62459	11.5	5.7	10.6
FN_3	-263.29092	8.3	-263.40485			
N_2	-109.26193	3.1	-109.3007			
FN_3+N_2	-372.55285	11.4	-372.70555	-48.3	-45.5	-46.0

* a. Basis set = 6-31+G(d), b. Basis set = aug-cc-pVDZ, c. Basis set = aug-cc-pVDZ
d. Includes ZPE correction
e. TS notation: TS2p = cis(2)→ FN_3 + N_2
TS14 = bifurcated(1) → harp(4)
TS42 = harp(4)→ cis(2)
TS4p = harp(4)→ FN_3 + N_2

Table 4. Distances, angles, and dihedral angles for FN_5 isomers-MP2/6-31+G(d)(refer to Figure 5).

	Distances (Å)							
Isomer	N1-N2	N2-N3	N3-N4	N4-N5	F-N1	F-N2	F-N3	F-N4
bifurcated	1.166	1.339	1.308	1.147	--	1.837	2.459	2.179
cis	1.239	1.396	1.279	1.152	1.452			
trans	1.251	1.404	1.275	1.152	1.416			
harp	1.233	1.362	1.293	1.157	1.495			
wag	1.253	1.393	1.285	1.156	1.412			
cyclic	1.318	1.337	1.351	1.337	1.345			

	Angles (degrees)			
Isomer	F-N1-N2	N1-N2-N3	N2-N3-N4	N3-N4-N5
bifurcated	--	137.78	109.38	160.37
cis	112.16	117.42	107.54	169.77
trans	107.39	107.33	170.27	104.98
harp	129.23	119.27	162.54	112.42
wag	106.25	112.88	114.85	169.22
cyclic	121.29	101.59	109.70	109.70

	Dihedral (degrees)		
Isomer	F-N1-N2-N3	N1-N2-N3-N4	N2-N3-N4-N5
bifurcated	180	180	180
cis	0	180	180
trans	180	180	180
harp	0	0	180
wag	180	0	180
cyclic	180	0	0

Table 5. Distances, angles, and dihedral angles for FN_5 transition states-MP2/6-31+G(d) (refer to Figure 6).

	Distances(Å)							
Molecule	N1-N2	N2-N3	N3-N4	N4-N5	F-N1	F-N2	F-N3	F-N4
TS14	1.144	1.315	1.356	1.16	2.022	2.351	2.716	2.049
TS2p	1.248	1.27	1.675	1.138	1.489			
TS42	1.230	1.448	1.264	1.155	1.495			
TS4p	1.242	1.264	1.563	1.142	1.509			

	Angles (degrees)			
Molecule	F-N1-N2	N1-N2-N3	N2-N3-N4	N3-N4-N5
TS14	91.62	150.36	107.04	145.03
TS2p	107.44	125.92	106.07	150.15
TS42	113.49	118.76	109.55	171.99
TS4p	108.68	138.9	113.77	152.47

	Dihedral (degrees)		
Molecule	F-N1-N2-N3	N1-N2-N3-N4	N2-N3-N4-N5
TS14	0	0	180
TS2p	0	180	180
TS42	7.33	-92.57	-172.06
TS4p	0	0	180

Table 6. Activation energies (kcal/mol) for isomerization and decomposition reactions

Barriers	$\Delta E(MP2/G)^{a,d}$	$\Delta E(CCSD(T))^{b,d}$	$\Delta E(MP2/aug)^{c,d}$
TS14	18.8	8.9	18.1
TS42	5.4	3.7	5.5
TS2p	21.8	13.2	21.6
TS4p	7.5	1.0	6.9

* a. Basis set = 6-31+G(d), b. Basis set = aug-cc-pVDZ, c. Basis set = aug-cc-pVDZ
d. Includes ZPE correction

Table 7. Vibrational frequencies and corresponding IR intensities for FN_5 isomers and transition states in the isomerization/decomposition PES surfaces (MP2/6-31+G(d))

Molecule	Frequencies, cm^{-1} (IR intensities, $debye^2/amu\text{-}ang^2$)
bifurcated (1)	130(0.032), 232(0.415), 316(0.479), 418(0.048), 460(0.084), 541(1.693), 565(0.308), 669(0.984), 1007(2.234), 1212(2.616), 1965(5.003), 2269(2.992)
cis (2)	113(0), 178(0.044), 300(0.190), 485(0.064), 554(0.001), 638(0.122), 691(3.290), 822(2.306), 999(1.784), 1196(3.807), 1532(1.153), 2321(9.337)
trans (3)	122(0.001), 164(0.044), 340(0.075), 399(0.226), 460(0.047), 521(0.185), 716(0.321), 947(4.070), 1050(0.308), 1220(4.531), 1481(0.069), 2356(8.660)
harp (4)	49(0.016), 221(0.006), 315(0.533), 452(0.091), 518(1.043), 546(0.001), 721(1.974), 860(0.785), 916(0.790), 1139(2.967), 1546(2.382), 2175(6.153)
wag (5)	146(0.005), 148(0.010), 361(0.023), 395(0.396), 472(0.092), 517(0.012), 766(2.388), 988(0.448), 1024(2.399), 1123(4.000), 1443(0.102), 2252(5.988)
cyclic (6)	272(0.052), 435(0.045), 614(0.002), 701(0.143), 727(0), 1022(0.018), 1034(0.198), 1090(0.088), 1132(0.024), 1211(0.175), 1378(0.134), 1387(1.832)
TS14	493 i, 115, 307, 391, 423, 456, 516, 701, 898, 1120, 1901, 2311
TS4p	823 i, 115, 159, 328, 335, 442, 591, 699, 807, 1206, 1550, 1993
TS42	109 i, 204, 310, 446, 500, 611, 724, 806, 864, 1230, 1538, 2409
TS2p	728 i, 86, 125, 242, 265, 444, 581, 706, 823, 1111, 1505, 2046

Table 8. RRKM analysis for isomerization and decomposition reactions as a function of excess energy

Bifurcated—TS14—harp Excess Energy (kcal/mol)	E[CCSD(T)] [b,c] (kcal/mol)	E[MP2/G] [a,c] (kcal/mol)	CCSD(T) lifetime	MP2/G lifetime
5	13.9	23.8	5.5 ns	1.9 μs

10	18.9	28.8	78.3 ps	7.6 ns
20	28.9	38.8	4.0 ps	100.9 ps
30	38.9	48.8	1.2 ps	14.6 ps
40	48.9	58.8	0.6 ps	4.8 ps

Harp—TS42--cis

Excess Energy (kcal/mol)	E[CCSD(T)] [b,c] (kcal/mol)	E[MP2/G] [a,c] (kcal/mol)	CCSD(T) lifetime	MP2/G lifetime
5	8.7	10.4	0.3 ns	2.1 ns
10	13.7	15.4	23.1 ps	78.7 ps
20	23.7	25.4	4.6 ps	9.5 ps
30	33.7	35.4	2.5 ps	4.3 ps
40	43.7	45.4	1.9 ps	2.8 ps

Harp—TS4p--FN_3+N_2

Excess Energy (kcal/mol)	E[CCSD(T)] [b,c] (kcal/mol)	[MP2/G] [a,c] (kcal/mol)	CCSD(T) lifetime	MP2/G lifetime
5	6.0	12.5	0.3 ps	0.9 ns
10	11.0	17.5	0.1 ps	18.3 ps
20	21.0	27.5	67.0 fs	1.3 ps
30	31.0	37.5	56.0 fs	451.4 fs
40	41.0	47.5	51.2 fs	256.8 fs

Cis—TS2p—FN_3+N_2

Excess Energy (kcal/mol)	E[CCSD(T)] [b,c] (kcal/mol)	E[MP2/G] [a,c] (kcal/mol)	CCSD(T) lifetime	MP2/G lifetime
5	18.2	26.8	7.2 ns	480.2 ns
10	23.2	31.8	50.1 ps	1.5 ns
20	33.2	41.8	1.3 ps	15.3 ps
30	43.2	51.8	0.3 ps	1.9 ps
40	53.2	61.8	0.1 ps	0.6 ps

* a. Basis set = 6-31+G(d), b. Basis set = aug-cc-pVDZ, c. Includes ZPE correction

Table 9. RRKM analysis for isomerization and decomposition reactions, as a function of vibrational quanta

Harp—TS42—cis
Mode 12 (harp)

Applied energy (quanta)	E (kcal/mol)	CCSD(T) [b] lifetime	MP2/G [a] lifetime
1	6.21	18.2 ns	2.5 ms
2	12.42	36.2 ps	353.0 ps

3	18.63	8.2 ps	29.3 ps
4	24.84	4.2 ps	10.1 ps
5	31.05	2.9 ps	5.6 ps
6	37.26	2.2 ps	3.9 ps
7	**43.47**	**1.9 ps**	**3.0 ps**
8	49.68	1.6 ps	2.4 ps
9	55.89	1.5 ps	2.1 ps
10	62.1	1.4 ps	1.9 ps
11	68.31	1.3 ps	1.7 ps
12	74.52	1.2 ps	1.6 ps
13	80.73	1.2 ps	1.5 ps
14	86.94	1.1 ps	1.4 ps
15	93.15	1.1 ps	1.3 ps

Harp—TS4p—FN_3+N_2
Mode 12 (harp)

Applied energy (quanta)	E (kcal/mol)	CCSD(T)[b] lifetime	MP2/G[a] lifetime
1	6.21	0.3 ps	--
2	12.42	99.5 fs	1.0 ns
3	18.63	72.0 fs	11.2 ps
4	24.84	61.5 fs	2.0 ps
5	31.05	56.0 fs	811.5 fs
6	37.26	52.6 fs	459.4 fs
7	**43.47**	**50.4 fs**	**311.4 fs**
8	49.68	48.7 fs	234.6 fs
9	55.89	47.5 fs	189.2 fs
10	62.1	46.5 fs	159.8 fs
11	68.31	45.8 fs	139.4 fs
12	74.52	45.1 fs	124.6 fs
13	80.73	44.6 fs	113.3 fs
14	86.94	44.2 fs	104.6 fs
15	93.15	43.8 fs	97.6 fs

* a. Basis set = 6-31+G(d), b. Basis set = aug-cc-pVDZ

Cis—TS2p—FN_3+N_2
Mode 10 (cis)

Applied energy (quanta)	E (kcal/mol)	CCSD(T)[b] lifetime	MP2/G[a] lifetime
1	3.49	---	---
2	6.98	---	---
3	10.47	---	---
4	13.96	855.1 ms	---
5	17.45	30.0 ns	---
6	20.94	0.3 ns	---

7	24.43	25.4 ps	0.2 ms
8	27.92	5.5 ps	77.1 ns
9	31.41	1.9 ps	2.0 ns
10	**34.9**	**891.3 fs**	**215.8 ps**
11	38.39	491.2 fs	46.2 ps
12	41.88	306.0 fs	14.8 ps
13	45.37	208.2 fs	6.1 ps
14	48.86	151.3 fs	3.0 ps
15	**52.35**	**115.5 fs**	**1.7 ps**

* a. Basis set = 6-31+G(d), b. Basis set = aug-cc-pVDZ

Figure 1. N_5^+ Resonance structures

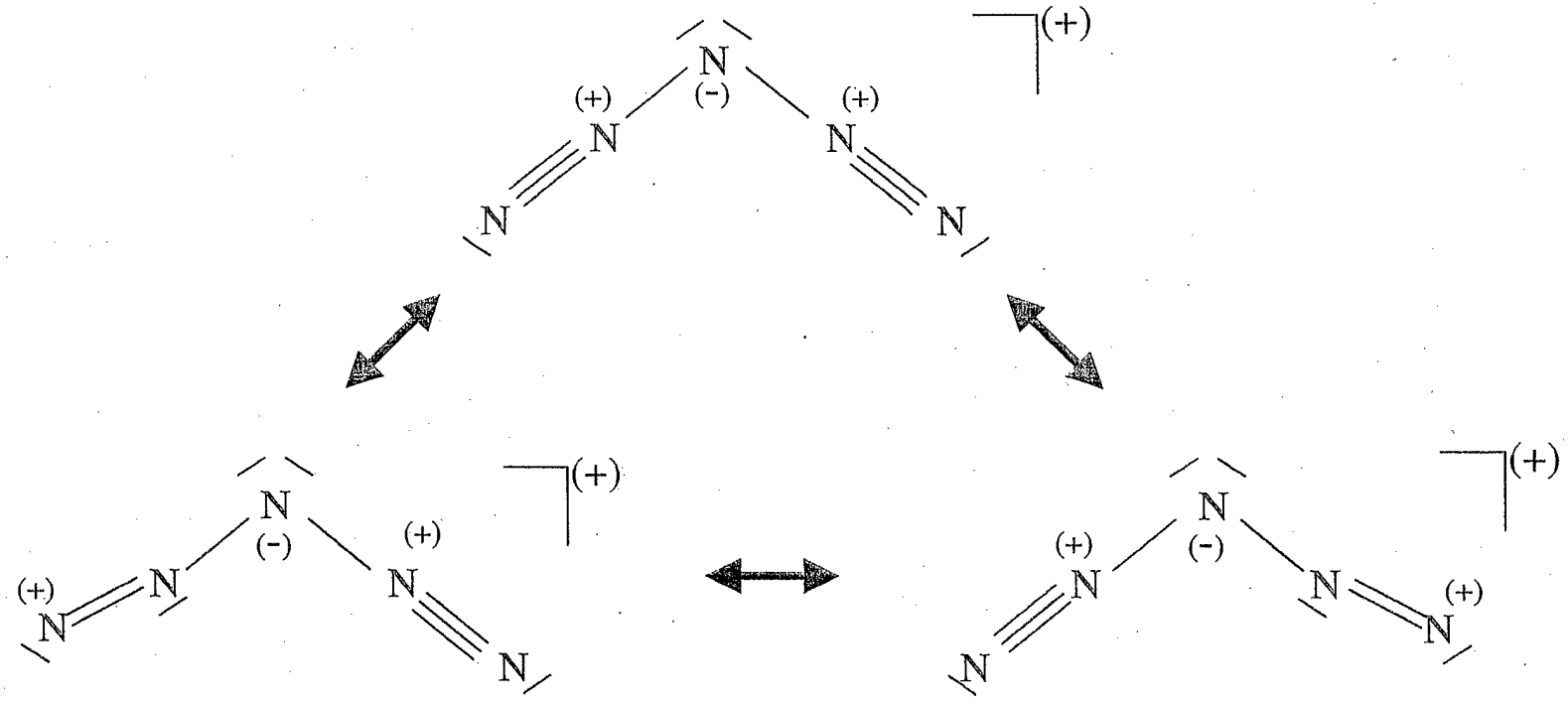

Figure 2. Optimized ion pair complex, $[N_5]^+[AsF_6]^-$

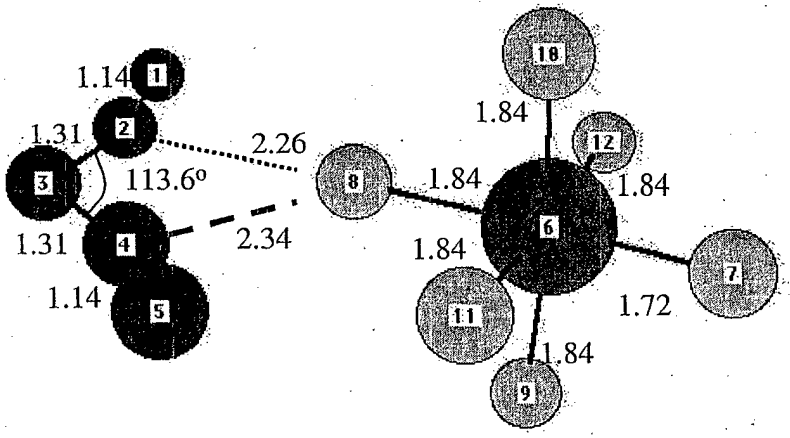

a. Bond distances (Å) and angles

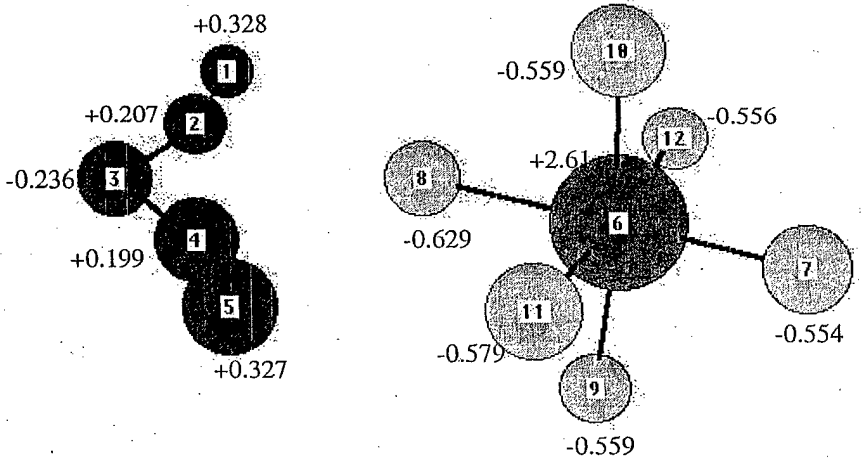

b. Mulliken charges

Figure 3. Separated Ions, N_5^+ and AsF_6^-

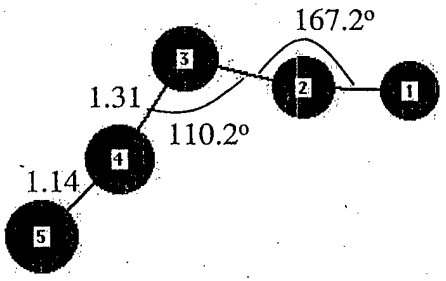

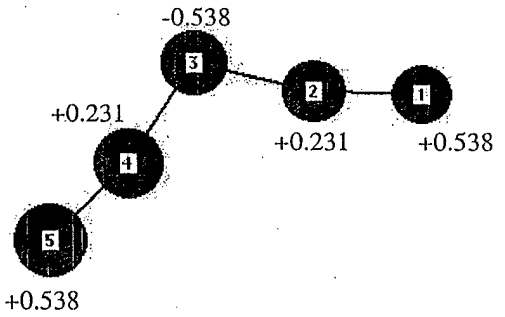

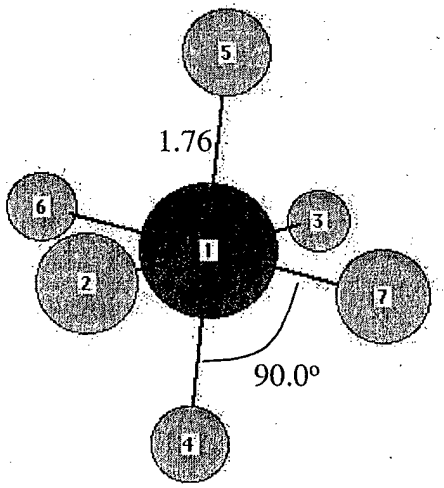

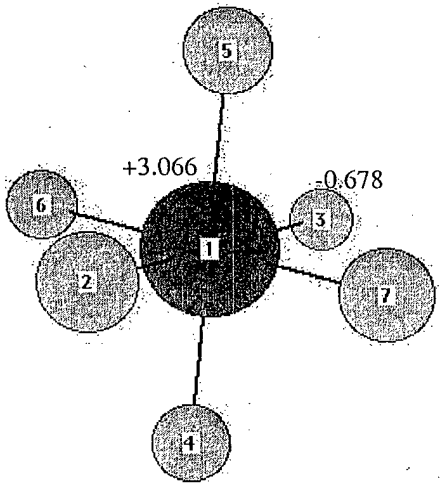

a. Bond distances (Å) and angles

b. Mulliken charges

Figure 4. Relative energy diagram (kcal/mol): ion complex, separated ions, and separated neutrals (reference = ion complex)

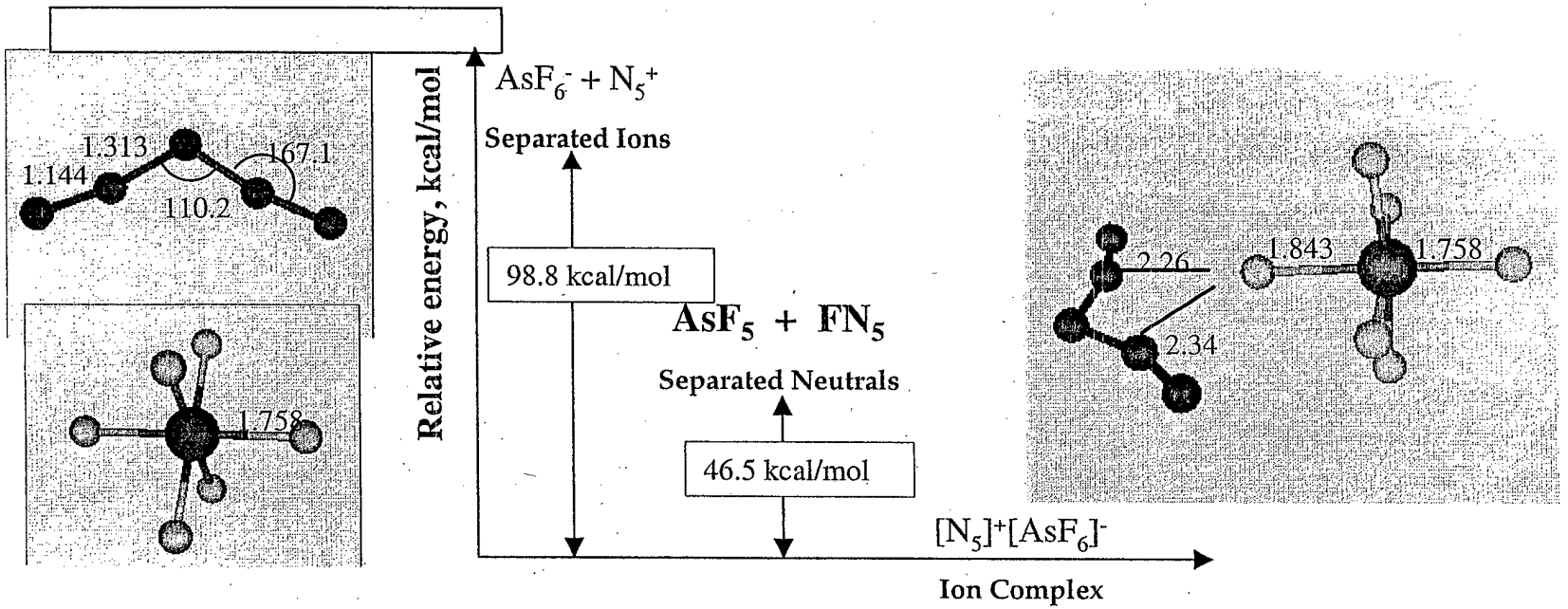

*Energies: MP2/6-31++G(d,p)

Figure 5. FN_5 isomers (MP2/6-31++G(d,p) geometries)

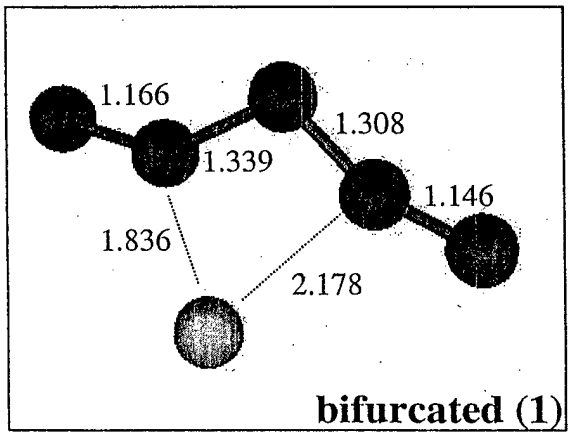

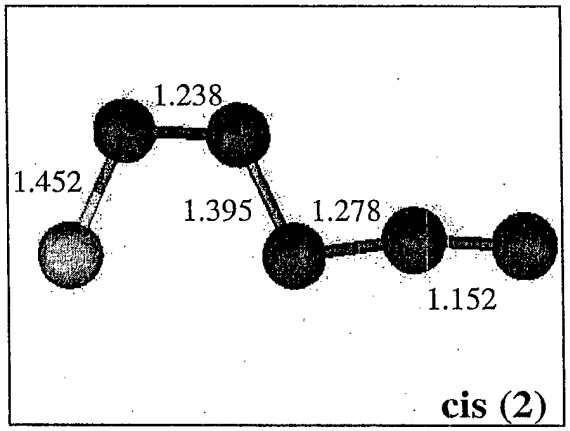

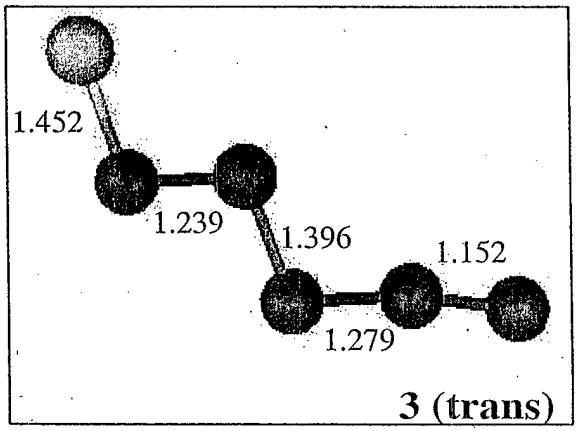

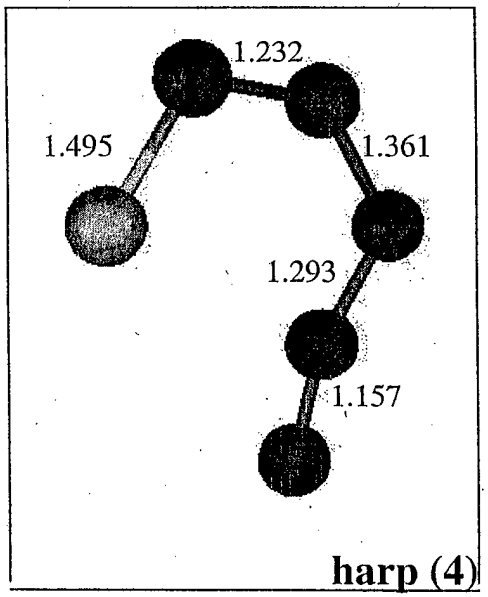

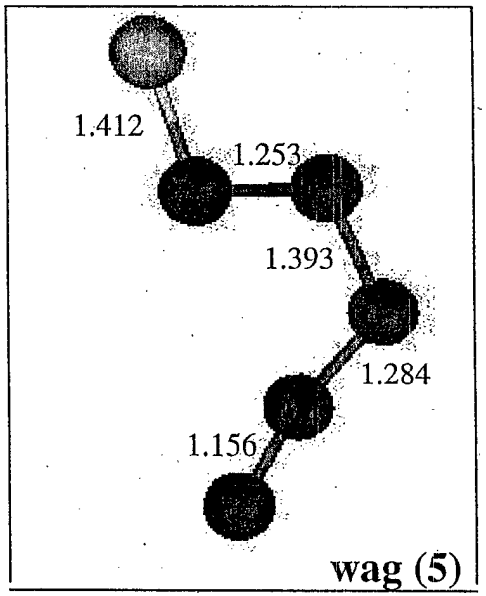

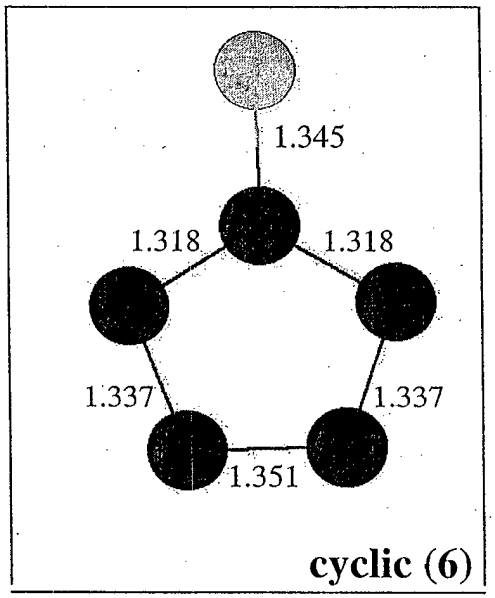

*Bond distances in Å

Figure 6. FN_5 transition states (MP2/6-31++G(d,p) geometries)

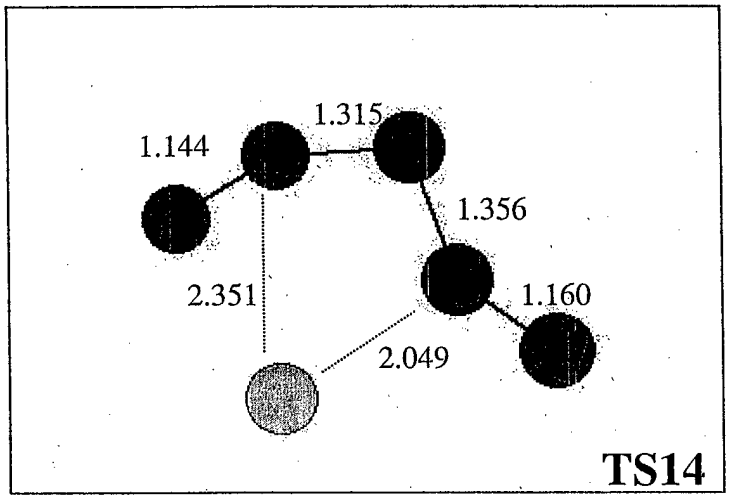

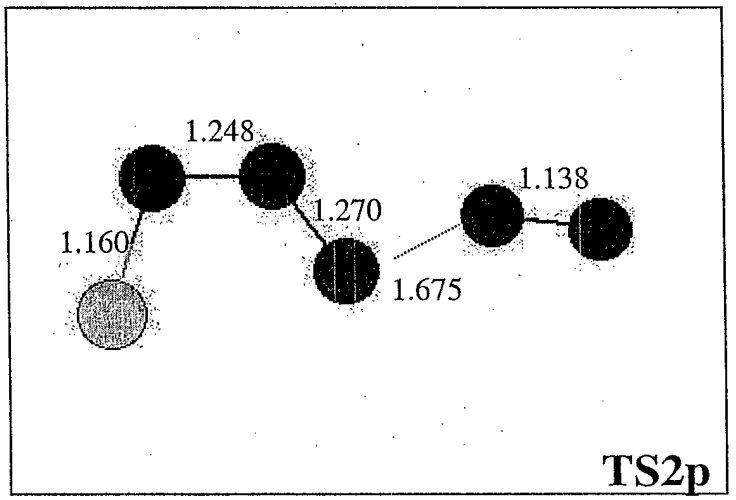

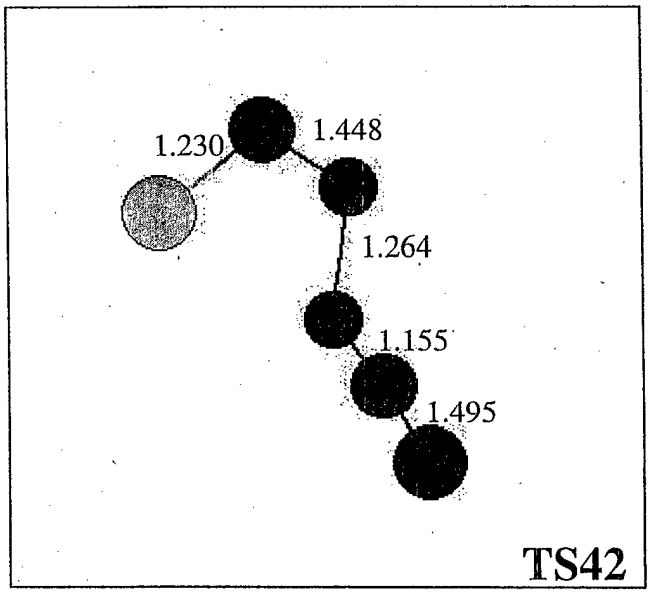

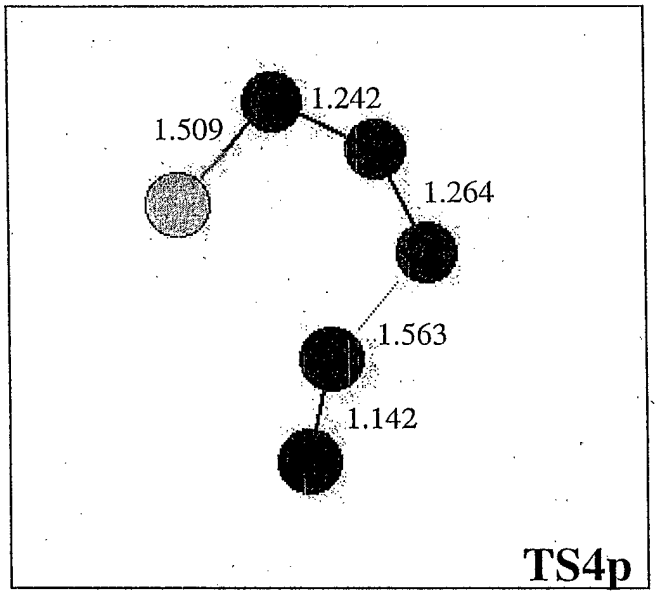

*Bond distances in Å

Figure 7. Optimized FN_3 and N_2 (MP2/6-31++G(d,p) geometries)

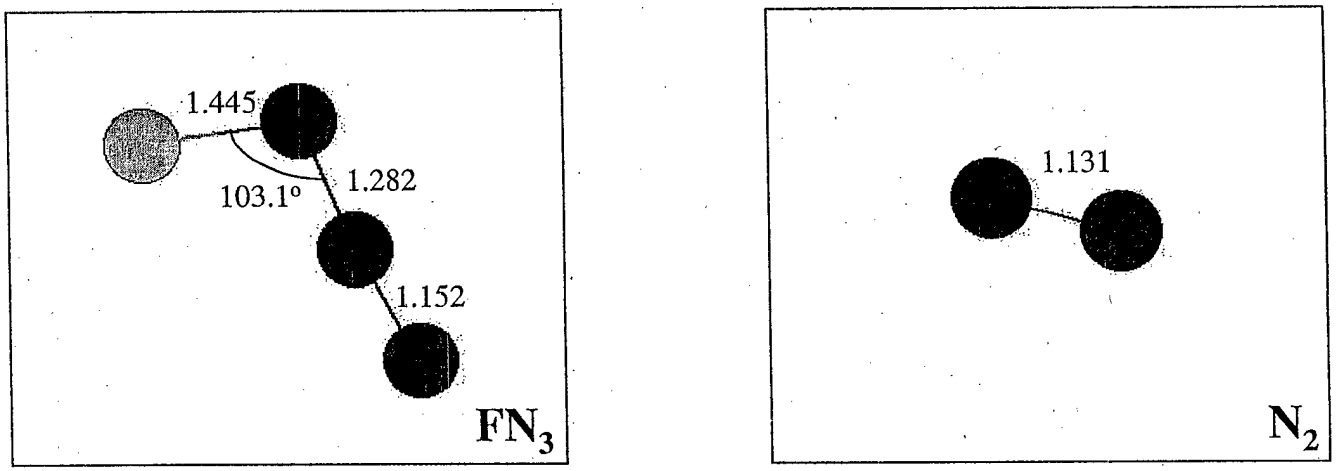

*Bond distances in Å

Figure 8. Relative isomerization/decomposition PESs with FN_5 isomers (reference = cis isomer)

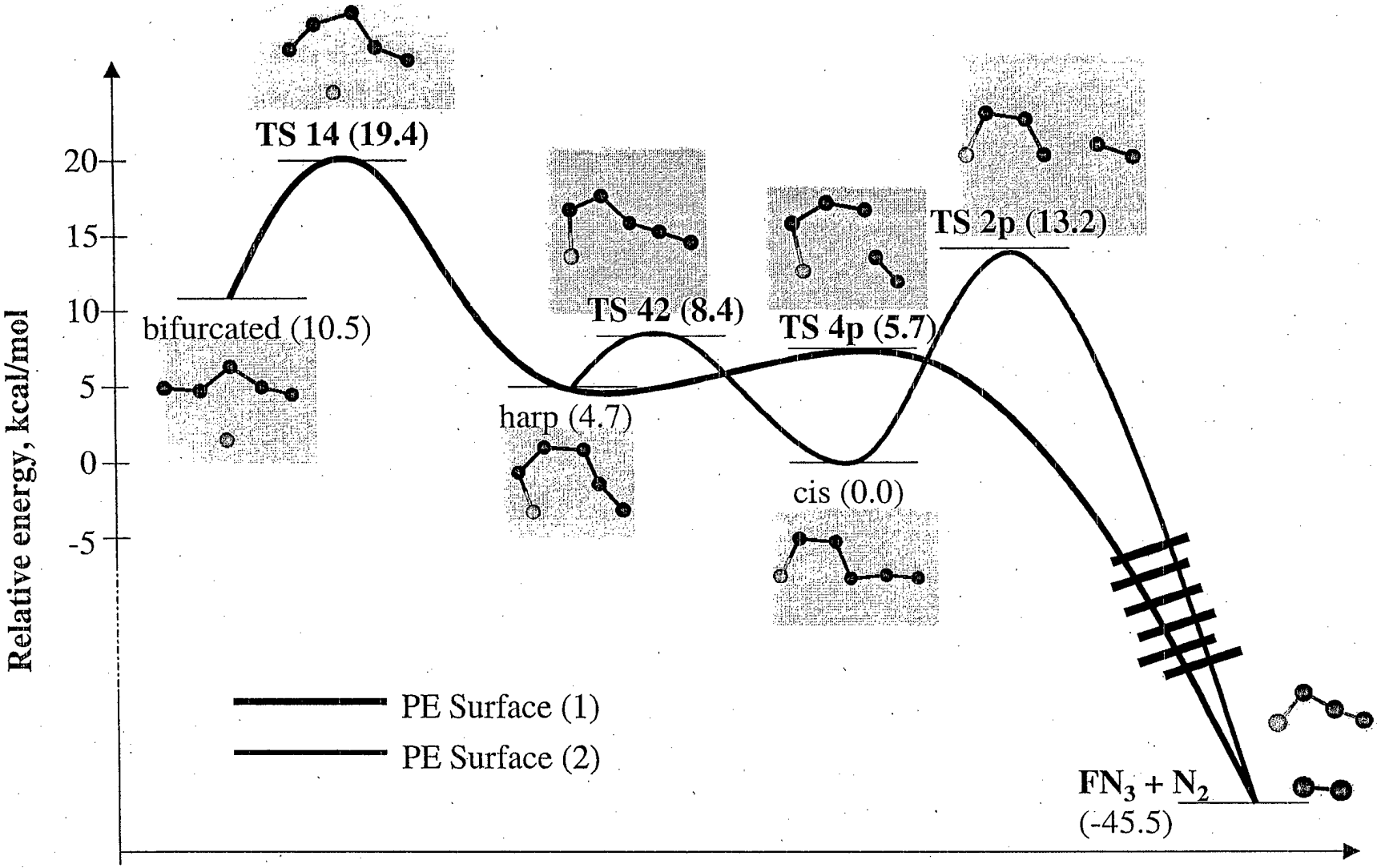

*Energies: CCSD(T)/aug-cc-pVDZ with ZPE

Figure 9.

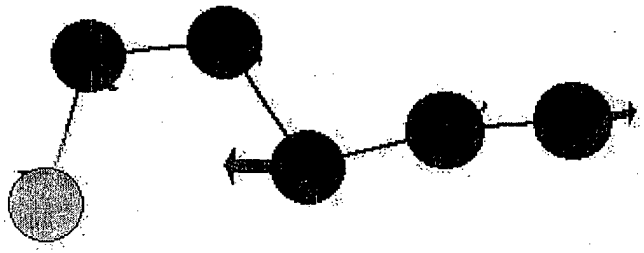

a. cis: inverted mode 10

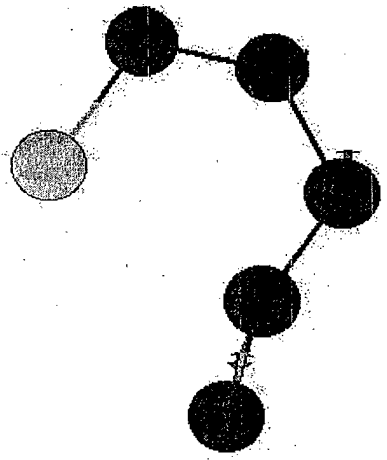

b. harp : inverted mode 12

Figure 10. Stages along the trajectory for adding an initial KE of 34.9 kcal/mol to mode 10, cis isomer

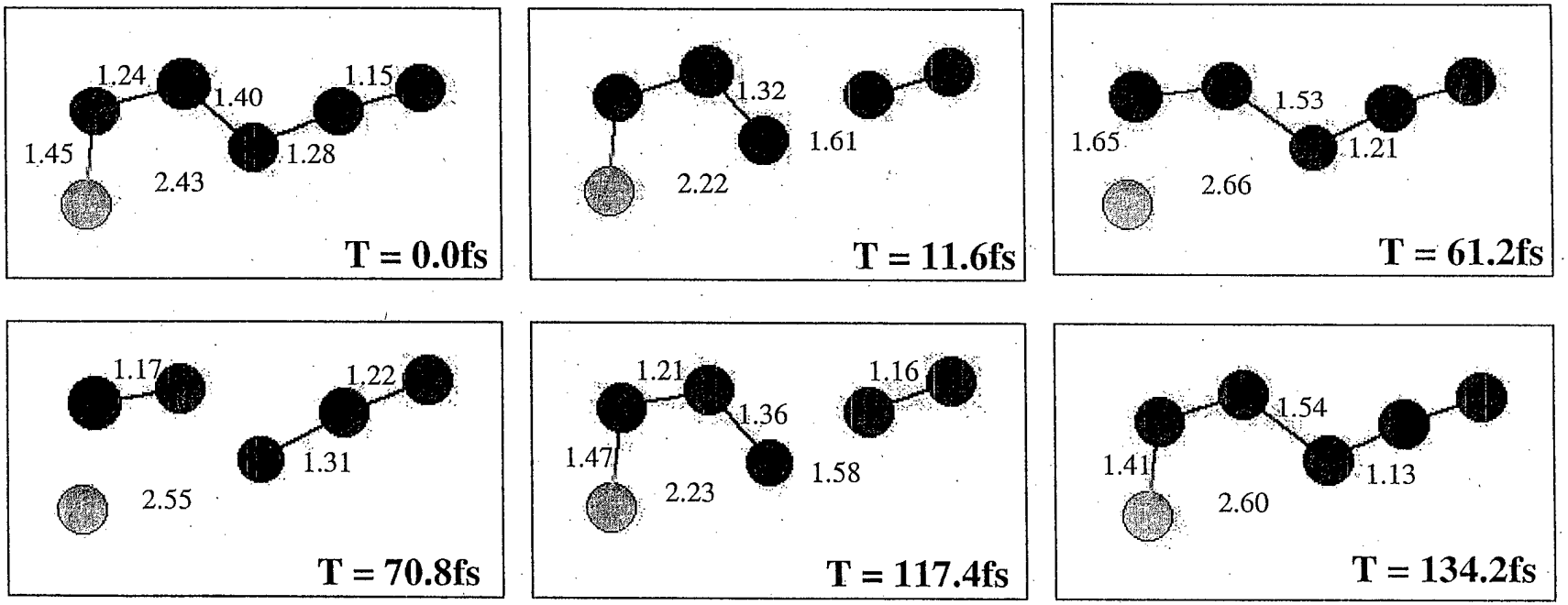

*Distances in Å(bond lengths shown have changed by > 0.40 Å)

Figure 11. Stages along the trajectory for adding an initial KE of 51.3 kcal/mol to mode 10, cis isomer

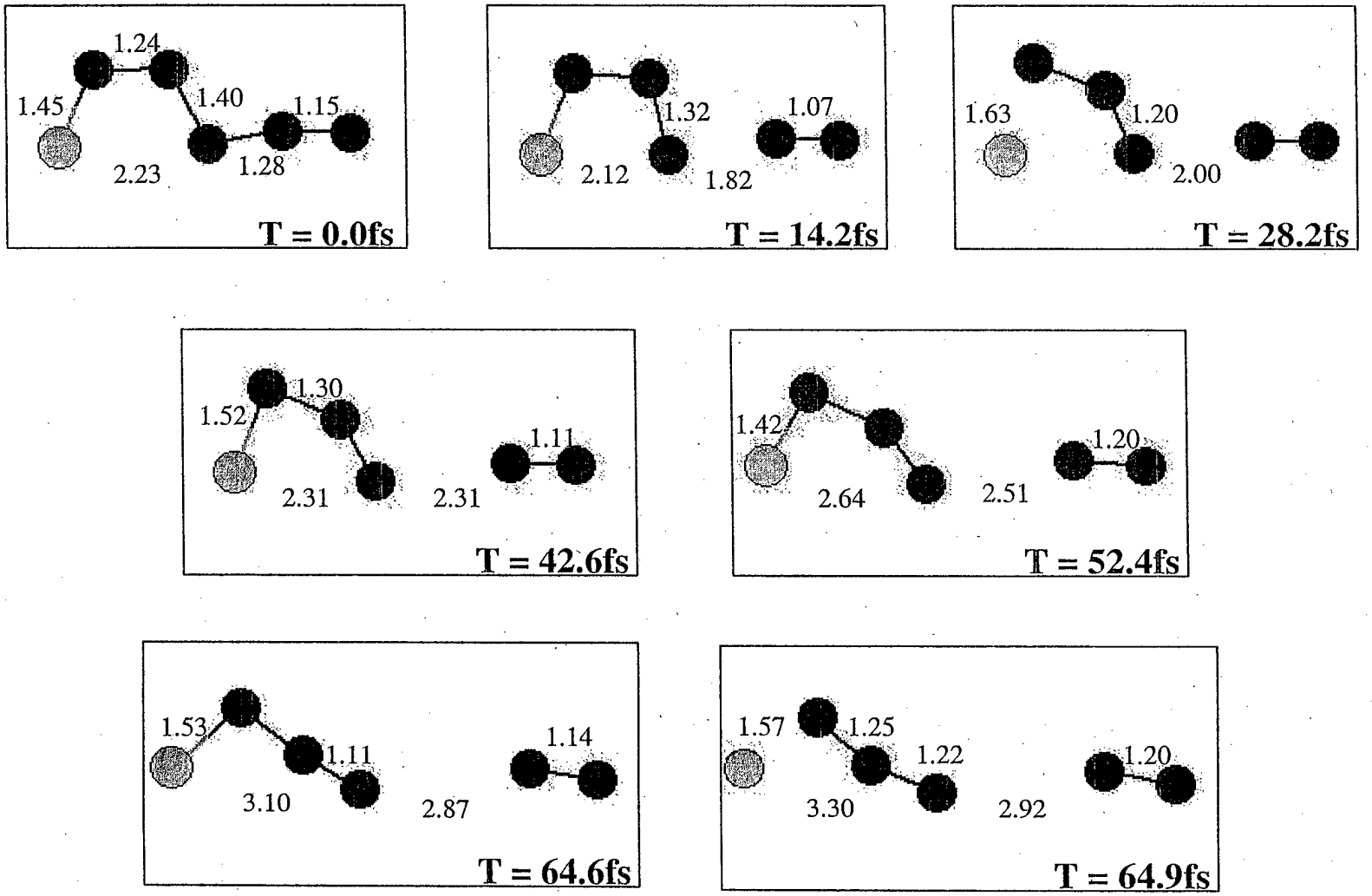

Figure 12. Normal coordinate change for cis isomer: Addition of KE to mode 10

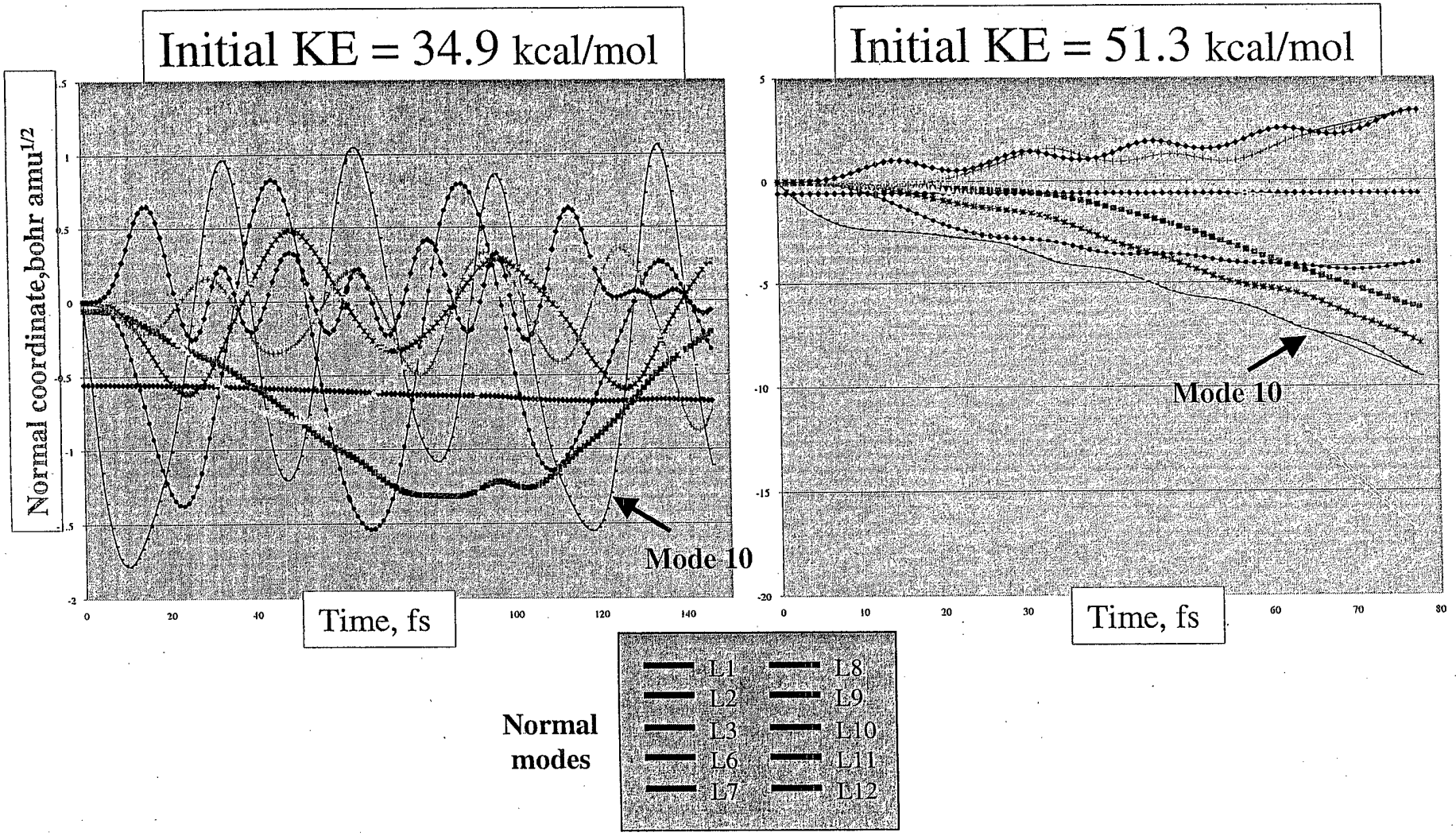

Figure 13. Normal coordinate change for harp isomer: Addition of KE to mode 12